Modeling and Control of a Nonholonomic Wheeled Mobile Robot with Wheel Slip Dynamics

Yu Tian, Naim Sidek and Nilanjan Sarkar Senior *Member, IEEE*

***Abstract*—In order to model a Wheeled Mobile Robot (WMR) system to improve its maneuverability in a real environment, wheel dynamics, which may violate no-slipping and pure rolling constraints, needs to be studied. In this paper, wheel dynamics with slip is modeled and introduced into the robot overall dynamics. Wheel slip phenomenon is captured and at the same time accommodated. Considering both lateral and longitudinal slip phenomena due to traction, a WMR system becomes an underactuated dynamic system. A time-invariant discontinuous feedback law is developed to asymptotically stabilize the system to the desired configuration with exponential convergence rate. Simulation results are provided to validate the theoretical results.**

1 Introduction

As holonomic WMRs have been increasingly applied in high speed operation in unstructured environment, wheel slip becomes an issue when ideal rolling assumption is not satisfied. In ideal rolling constraint, the wheels of a mobile robot are assumed to roll without slipping. This ideal rolling constraint is violated when the robot is either accelerating, or decelerating, or corning at a high speed. If the slip is not considered, a designed task may not be completed and a stable system may even become unstable due to the slip.

There are a few recent papers that present approaches to model wheel slips. [1] was one of the earliest work where slip was considered in the WMR dynamic model. The authors took into account small values of slip ratios on which traction force is linearly dependent. Then they developed a slow manifold approach to design output feedback control law. [2] introduced anti-slip factor to represent the percentage of a wheel's angular velocity that reflects the wheel's forward speed. This same factor also represents the percentage of the wheel's driving force reflected effectively by the road friction. The road friction was considered as unmodelled dynamics. Neural network technique was applied to realize optimal velocity tracking control. In [3][4] the slip states were introduced into a generalized WMR kinematic model. In [5] slip was considered as a small, measurable, bounded disturbance in the WMR kinematic model. And a kinematic control law was developed to overcome the disturbance. In [6] longitudinal traction force was included in an omini-directional WMR model by externally measuring the magnitude of slip. In [7] lateral traction force was introduced which is linearly dependent on lateral slip, and applied a steering control approach to lateral position tracking control for a bicycle model. In [8] longitudinal slip dynamics was considered in an omni-directional WMR model. However in the control input derivation, pure rolling was assumed to obtain ideal relationship between driving torque and traction force. In [9] both longitudinal and lateral traction were introduced which approximately linearly dependent on longitudinal and lateral slip, respectively, for a reduced unicycle model for a 4WD robot. In the controller, slips and steering torque were control input to be designed first, and then by assuming tire dynamics was significantly faster than WMR dynamics, drive torque was designed to control slips.

In our previous work [10], lateral wheel slip dynamics was explicitly modeled in a WMR's overall dynamics, and input-output feedback control law was applied to accomplish designed path following task. In this paper, we model both lateral and longitudinal wheel slips in a dynamic way. When both slip dynamics are introduced into robot overall dynamic model, the overall robot model becomes a third order underactuated dynamic system with second order nonholonomic constraints, which will be observed in later sections. Such a model is quite different from typical ideal WMR's dynamic model. Therefore those control approaches for an ideal robot dynamic model, such as backstepping technique in [11][12][13], observer based controller in [14], cannot be applied to this non-ideal model.

However this model is similar to underactuated surface vessel models in literature. To control such a system, researchers have developed various controllers in the past decade. In [15] discontinuous coordinate transformation named σ-process was applied to transform an underactuated surface vessel model to a form where linear state feedback control law is able to be designed to stabilize the system to desired configuration with exponential convergence rate. In [16][17][18] surface vessel model was transformed to a chained form where either discontinuous or time-varying feedback control law can be designed to asymptotically converge the system to zero. In [19][20] tracking control law was developed for underactuated surface vessel. To control the robot model we developed, we apply σ-process to transform the model because our model has more nonlinear terms and cannot be represented in a chained form as in [16][17][18]. Then we design linear feedback law to control the transformed system to converge to desired configuration.

The remainder of this article is organized as follows. Section 2 provides theoretical background of a nonholonomic WMR model with and without slip dynamics. In section 3 we transform the system to a new form by applying σ-process, and design feedback control law for the new form. Section 4

Yu Tian and Nilanjan Sarkar are with the Mechanical Engineering Department, Vanderbilt University, Nashville, TN 37209 USA. (e-mail: yu.tian@vanderbilt.edu, nilanjan.sarkar@vanderbilt.edu).

Naim Sidek is with the Electrical Engineering Department, Vanderbilt University, Nashville, TN 37209 USA. (e-mail: naim.sidek@gmail.com).

978-1-4244-2752-9/09/$25.00 ©2009 IEEE

presents some simulation results. Finally section 6 gives conclusion remarks and directions of future work.

2 NONHOLONOMIC WMR MODELLING

2.1. A nonholonomic WMR without wheel slips— ideal model

A nonholonomic WMR system having n-dimensional configuration space L with generalized coordinates $(q_1,\ldots,q_n)$ and subject to m constraints can be described by [21][22][23][24][25][1][8]

$$M(q)\ddot{q} + C(q,\dot{q}) = B(q)u + A^T(q)\lambda \qquad (1)$$

where $q \in \Re^{n\times 1}$ is a vector of generalized coordinates and $\dot{q} \in \Re^{n\times 1}$ is a vector of linear and angular velocities along generalized coordinates. $M(q) \in \Re^{n\times n}$ is a symmetric positive definite inertia matrix of the system. $C(q,\dot{q}) \in \Re^{n\times 1}$ is the centrifugal and Coriolis force vector. $B(q) \in \Re^{n\times(n-m)}$ and $u \in \Re^{(n-m)\times 1}$ are the input transformation matrix and input vector, respectively. $\lambda \in \Re^{m\times 1}$ is a vector of *Lagrange* multipliers and $A^T\lambda$ corresponds to the constraint forces related to the kinematic constraints. The constraint equations can be defined as,

$$A(q)\dot{q} = 0 \qquad (2)$$

where $A(q) \in \Re^{m\times n}$ is a matrix associated with the kinematic constraints of the nonholonomic system.

Let S(q) be a full rank matrix (n-m) formed by a set of smooth and linearly independent vector fields spanning the null space of $A(q)$, i.e.,

$$S(q)^T A(q)^T = 0 \qquad (3)$$

According to (2) and (3), it is possible to find an auxiliary vector function $v(t) \in \Re^{(n-m)\times 1}$ such that for all t,

$$\dot{q}(t) = S(q)v(t) \qquad (4)$$

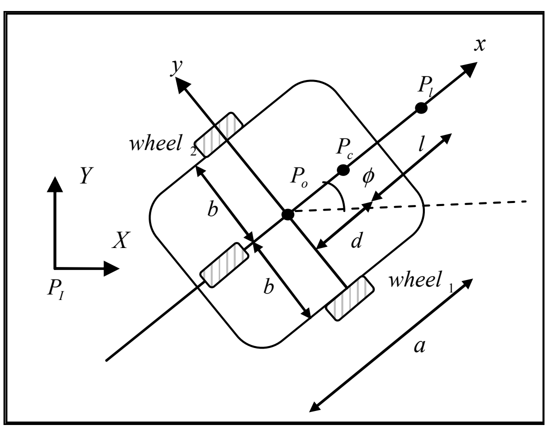

Fig. 1 Two-wheeled nonholonomic mobile robot system

The mobile robot shown in Figure 1 is our nonholonomic robot system. It consists of a vehicle, two driving wheels mounted along same axis, and one caster wheel. The motion of the robot is determined by two independent actuators, e.g., DC motors providing torque to the two driving wheels. The center of mass (COM) of the robot is located at point P_c and P_l is defined as a look-ahead point located on the x -axis of the WMR body frame. Point P_o is the origin of WMR axis, which is located at the intersection of the x-axis and y-axis of the body frame. a and $2b$ are the length and the width of the WMR body, respectively. d is the distance from point P_o to point P_c. The distance from P_c to the look-ahead point is l. The radius of each wheel is r. In the inertial frame $\{X, Y\}$, the degree of freedom of the robot is represented by a vector of generalized coordinates,

$$q = [x_c, y_c, \phi, \theta_1, \theta_2]^T \qquad (5)$$

where x_c and y_c are the coordinates of the COM of the robot. ϕ denotes the orientation of the frame on the WMR with respect to the inertial frame, and $[\theta_1, \theta_2]$ is the angular displacement vector of the two driving wheels *wheel*$_1$ and *wheel*$_2$, respectively.

With the pure rolling and no-slipping assumption in the ideal robot model, the following nonholonomic constraints hold,

$$r\dot{\theta}_1 = \dot{x}_c \cos\phi + \dot{y}\sin\phi + b\dot{\phi}$$

$$r\dot{\theta}_2 = \dot{x}_c \cos\phi + \dot{y}\sin\phi - b\dot{\phi} \qquad (6)$$

$$0 = \dot{y}_c \cos\phi - \dot{x}_c \sin\phi - d\dot{\phi} \qquad (7)$$

where (6) is the pure rolling constraint meaning that the forward velocity of the WMR is uniquely determined by the angular velocity of the two driving wheels, and (7) is the no-slipping constraint in lateral direction meaning that the lateral velocity of the WMR is always constrained to be zero.

Having above constraints, we can find matrix *S(q)* and auxiliary vector v in (4). Thus, differentiating (4) and substituting the result in (1), and then multiplying by S^T, we can eliminate the constraint term $A^T\lambda$. The complete equations representing the model of the nonholonomic mobile robot system are given by

$$\dot{q} = Sv \qquad (8)$$

$$(S^T MS)\dot{v} + S^T M\dot{S}v + S^T C = S^T Bu \qquad (9)$$

By appropriate definition we can write (9) as

$$\overline{M}(q)\dot{v} + \overline{C}(q,\dot{q})v = \overline{B}u \qquad (10)$$

where $\overline{M}(q)$ is a symmetric, positive definite inertia matrix, $\overline{C}(q,\dot{q})$ is the centrifugal and coriolis force matrix, $\overline{B}$ is a constant nonsingular matrix. Thus (9) describes the behavior of the nonholonomic system in a new set of local coordinates.

2.2. A nonholonomic WMR with wheel slips—non-ideal model

In this section, we relax the no-slipping condition by introducing new states due to wheel slips. We introduce ζ_i and η_i as the longitudinal and lateral slip displacement for the i-th wheel respectively.

We then define a new state ρ_i to represent the total longitudinal displacement of the wheel center as

$$\rho_i = r\theta_i - \zeta_i,$$

and our new generalized coordinates considering slips become

$$q = [x_c, y_c, \phi, \eta_1, \eta_2, \rho_1, \rho_2, \theta_1, \theta_2]^T$$

The new nonholonomic longitudinal constraints of the robot then become

$$\dot{\rho}_1 = \dot{x}_c \cos\phi + \dot{y}_c \sin\phi + b\dot{\phi}$$
$$\dot{\rho}_2 = \dot{x}_c \cos\phi + \dot{y}_c \sin\phi - b\dot{\phi} \tag{11}$$

Since the two driving wheels are rigidly connected with the robot body and do not have relative motion along lateral direction, their lateral slips have to be same, as seen below.

$$\dot{\eta}_1 = \dot{y}_c \cos\phi - \dot{x}_c \sin\phi - d\dot{\phi}$$
$$\dot{\eta}_2 = \dot{y}_c \cos\phi - \dot{x}_c \sin\phi - d\dot{\phi} \tag{12}$$

Writing above new constraints in the form of (2) and we will have A matrix as

$$A(q) = \begin{bmatrix} -\sin\phi & \cos\phi & -d & -1 & 0 & 0 & 0 & 0 & 0 \\ -\sin\phi & \cos\phi & -d & 0 & -1 & 0 & 0 & 0 & 0 \\ \cos\phi & \sin\phi & b & 0 & 0 & -1 & 0 & 0 & 0 \\ \cos\phi & \sin\phi & -b & 0 & 0 & 0 & -1 & 0 & 0 \end{bmatrix} \tag{13}$$

Then we can find matrix S and vector ν, which fulfill (3) and (4), as

$$S(q) = \begin{bmatrix} -\sin\phi & \dfrac{b\cos\phi - d\sin\phi}{2b} & \dfrac{b\cos\phi + d\sin\phi}{2b} & 0 & 0 \\ \cos\phi & \dfrac{d\cos\phi + b\sin\phi}{2b} & \dfrac{-d\cos\phi + b\sin\phi}{2b} & 0 & 0 \\ 0 & \dfrac{1}{2b} & -\dfrac{1}{2b} & 0 & 0 \\ 1 & 0 & 0 & 0 & 0 \\ 1 & 0 & 0 & 0 & 0 \\ 0 & 1 & 0 & 0 & 0 \\ 0 & 0 & 1 & 0 & 0 \\ 0 & 0 & 0 & 1 & 0 \\ 0 & 0 & 0 & 0 & 1 \end{bmatrix} \tag{14}$$

$\nu = [\dot{\eta}_2, \dot{\rho}_1, \dot{\rho}_2, \dot{\theta}_1, \dot{\theta}_2]^T$.

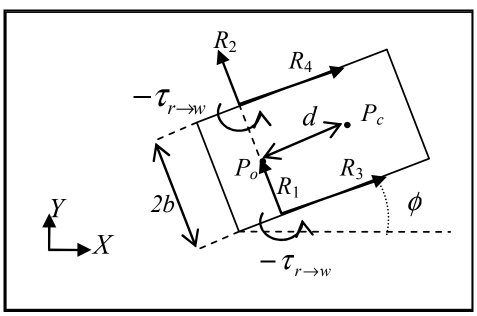

Fig.2 Free body diagram for robot body without wheels

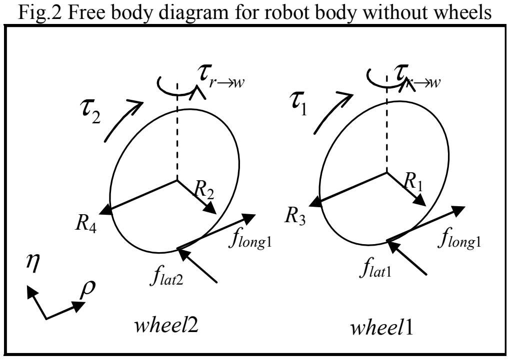

Fig. 3 Free body diagram for two driving wheels *wheel*1 and *wheel*2

Now we derive the dynamic model of the WMR system by free body diagram. From the free body diagram for robot body in Fig.3, we have first three dynamic equations in (15), knowing that $\tau_{r-w} = I_{wz}\ddot{\phi}$. From the free body diagram for two driving wheels in Fig.4, we have next four dynamic equations in (15) for translational wheel dynamics and last two dynamic equations in (15) for rotational wheel dynamics, by noting that $\ddot{\eta}_1$ and $\ddot{\eta}_2$ are translational lateral slip acceleration for *wheel*1 and *wheel*2, respectively, and $\ddot{\rho}_1$ and $\ddot{\rho}_2$ are translational longitudinal slip acceleration for *wheel*1 and *wheel*2, respectively.

X-Y **:** The world coordinate system;

ρ-η**:** The coordinate system fixed to each driving wheel's center

m_r**:** The mass of the robot platform without the driving wheels and the rotor of the DC motors;

m_w**:** The mass of each driving wheel plus the rotor of its motor;

I_{rz}**:** The moment of inertia of the robot platform without the driving wheels and the rotors of the motors about a vertical axis through P_c;

I_{wz}**:** The moment of inertia of each driving wheel and the motor rotor about a wheel diameter;

I_{wy}**:** The moment of inertia of each driving wheel and the motor rotor about the wheel axis;

R_i**:** The reaction forces between the robot body and two driving wheels;

$f_{lat1,2}$**:** The lateral traction force for each driving wheel;

$f_{long1,2}$**:** The longitudinal traction force for each driving wheel;

$\tau_{r\to w}$**:** The torque that the robot body gives to each driving wheel;

$\tau_{1,2}$ **:** The driving torque acting on each wheel axis generated by its motor;

P_c, P_0, b, d, r are defined as in subsection 2.1

$$\begin{cases} m_r\ddot{x}_c = -(R_1+R_2)\sin\phi + (R_3+R_4)\cos\phi \\ m_r\ddot{y}_c = (R_1+R_2)\cos\phi + (R_3+R_4)\sin\phi \\ (I_{rz}+2I_{wz})\ddot{\phi} = -(R_1+R_2)d + (R_3-R_4)b \\ m_w\ddot{\eta}_1 + m_w\dot{\phi}\dot{\rho}_1 = f_{lat1} - R_1 \\ m_w\ddot{\eta}_2 + m_w\dot{\phi}\dot{\rho}_2 = f_{lat2} - R_2 \\ m_w\ddot{\rho}_1 - m_w\dot{\phi}\dot{\eta}_1 = f_{long1} - R_3 \\ m_w\ddot{\rho}_2 - m_w\dot{\phi}\dot{\eta}_2 = f_{long2} - R_4 \\ I_{wy}\ddot{\theta}_1 = \tau_1 - f_{long1}r \\ I_{wy}\ddot{\theta}_2 = \tau_2 - f_{long2}r \end{cases} \tag{15}$$

If we write above equations in compact form, it will become

$$M(q)\ddot{q} + C(q,\dot{q}) = B(q)\tau + F(\dot{q}) + A^T(q)R \tag{16}$$

where inertia matrix M is,

$$M = diag\left[m_r, m_r, I_{rz}+2I_{wz}, m_w, m_w, m_w, m_w, I_{wy}, I_{wy}\right] \tag{17}$$

and vector C, consisting of centrifugal forces for the two wheels, is,

$$C = [0,0,0, m_w\dot{\phi}\dot{\rho}_1, m_w\dot{\phi}\dot{\rho}_2, -m_w\dot{\phi}\dot{\eta}_1, 0,0]^T \tag{18}$$

and vector R is,

$$R = [R_1 \quad R_2 \quad R_3 \quad R_4]^T \tag{19}$$

and matrix B is,

$$B = [0_{2\times7} \quad I_{2\times2}]^T \tag{20}$$

and the traction force vector is,

$$F(\dot{q}) = \left[0,0,0, f_{lat1}, f_{lat2}, f_{lon1}, f_{lon2}, -rf_{lon1}, -rf_{lon2}\right]^T \tag{21}$$

where each individual element of the traction force vector is calculated/generated from the magnitude of the respective slip.

Differentiating (4) and substituting into (16), and then multiplying by S^T, eliminating the term $A^T R$, we will have the robot dynamic equation as,

$$\left(S^T MS\right)\dot{v} + S^T M\dot{S}v + S^T C = S^T B\tau + S^T F \tag{22}$$

Writing (22) in another way, we can split (22) into two sets of equations as (23) and (24)

$$\left(\overline{S}^T \overline{MS}\right)\dot{\overline{v}} + \overline{S}^T \overline{M\dot{S}}\,\overline{v} + \overline{S}^T \overline{C} = \overline{S}^T \overline{F} \tag{23}$$

$$\begin{aligned} I_{wy}\ddot{\theta}_1 &= \tau_1 - rf_{lon1} \\ I_{wy}\ddot{\theta}_2 &= \tau_2 - rf_{lon2} \end{aligned} \tag{24}$$

where

$$\overline{M} = diag\left[m_r, m_r, I_{rz} + 2I_{wz}, m_w, m_w, m_w, m_w\right]$$

$$\overline{v} = [\dot{\eta}_2 \quad \dot{\rho}_1 \quad \dot{\rho}_2]^T$$

$$\overline{C} = [0,0,0, m_w\dot{\phi}\dot{\rho}_1, m_w\dot{\phi}\dot{\rho}_2, -m_w\dot{\phi}\dot{\eta}_1]^T$$

$$\overline{F} = \left[0,0,0, f_{lat\,1}, f_{lat\,2}, f_{lon\,1}, f_{lon\,2}\right]^T$$

$$\overline{S} = \begin{bmatrix} -\sin\phi & \dfrac{b\cos\phi - d\sin\phi}{2b} & \dfrac{b\cos\phi + d\sin\phi}{2b} \\ \cos\phi & \dfrac{d\cos\phi + b\sin\phi}{2b} & \dfrac{-d\cos\phi + b\sin\phi}{2b} \\ 0 & \dfrac{1}{2b} & -\dfrac{1}{2b} \\ 1 & 0 & 0 \\ 1 & 0 & 0 \\ 0 & 1 & 0 \\ 0 & 0 & 1 \end{bmatrix}$$

By appropriate definition we can write (23) as

$$\overline{\overline{M}}\dot{\overline{v}} + \overline{\overline{C}}(\overline{q}, \dot{\overline{q}})\overline{v} = \overline{\overline{F}} \tag{25}$$

where $\overline{\overline{M}}$ is a symmetric, positive definite constant inertia matrix, $\overline{q} = \left[x_c, y_c, \phi, \eta_1, \eta_2, \rho_1, \rho_2\right]^T$ and $\overline{C}(\overline{q}, \dot{\overline{q}})$ are the centrifugal and coriolis force matrix, respectively, and $\overline{\overline{F}}$ is the traction force vector. Rewrite (24) in a compact form as,

$$\overline{I}\dot{\Theta} = \overline{\tau} - r\overline{f} \tag{26}$$

where $\overline{I} = diag\left[I_{wy} \quad I_{wy}\right]$, $\Theta = \left[\dot{\theta}_1 \quad \dot{\theta}_2\right]^T$, $\overline{\tau} = \left[\tau_1 \quad \tau_2\right]^T$, and $\overline{f} = \left[f_{long1} \quad f_{long2}\right]^T$, the complete equations representing the robot's dynamic model with slips will be,

$$\begin{aligned} \dot{\overline{q}} &= \overline{S}\overline{v} \\ \overline{\overline{M}}\dot{\overline{v}} + \overline{\overline{C}}(\overline{q}, \dot{\overline{q}})\overline{v} &= \overline{\overline{F}} \\ \overline{I}\dot{\Theta} &= \overline{\tau} - r\overline{f} \end{aligned} \tag{27}$$

2.3. Traction force model

In this subsection we use the same traction model as in our previous work. We define slip ratio *sr* as a measure of percentage of the difference between the wheel's translational velocity generated by angular velocity only and the wheel's forward velocity at the hub, V_{wx} as formulated by

$$sr_i = \frac{r\dot{\theta}_i - \dot{\rho}_i}{\max(|r\dot{\theta}_i|, |\dot{\rho}_i|)} = \frac{\dot{\zeta}_i}{\max(|r\dot{\theta}_i|, |\dot{\rho}_i|)} \tag{28}$$

Meanwhile, we define slip angle *sa* as the angle between the instantaneous velocity and the longitudinal velocity of the wheel, formulated by

$$sa_i = a\tan\left(\frac{\dot{\eta}_i}{|\dot{\rho}_i|}\right) \tag{29}$$

The traction force model, thus, is generated from *Magic formula* using above slip variables. The model is represented in the form of (*http://www.miata.net/sport/Physics/*)

$$F = K_1 \sin\left(K_2 \tan^{-1}\left(SK_3 + K_4\left(\tan^{-1}\left(SK_3\right) - SK_3\right)\right)\right) + S_v \tag{30}$$

where S is a function of slip angle or slip ratio for lateral and longitudinal tractions, respectively. All the variables $K_i, i = 1,\ldots,4$ and S_v are constants and determined from the curve fitting process of the empirical data and can also be related to the tire characteristics. Fig.5 shows the traction force properties for two surfaces whose coefficient of friction are 0.7 and 0.3, respectively.

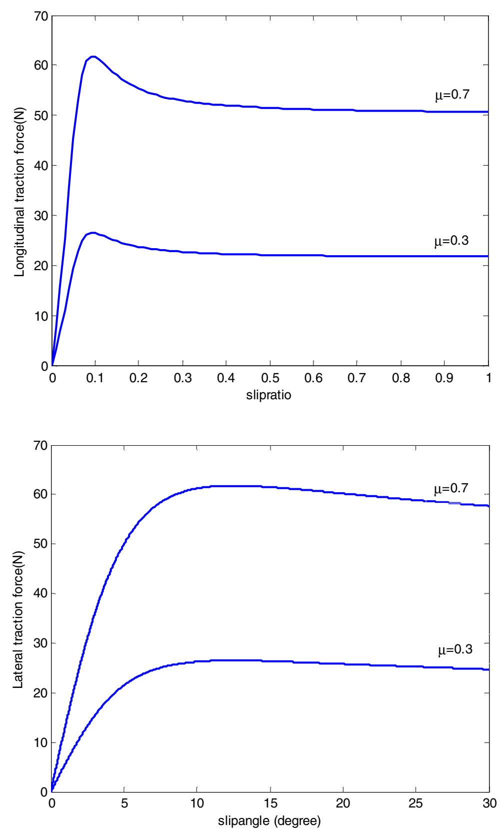

Fig.4 Traction force vs slipratio/slipangle relationship for two surfaces with different friction coefficients (a) 0.7 (b) 0.3

3. FEEDBACK CONTROLLER DESIGN

First we assume both slip ratio and slip angle are quite small and thus the traction force in (30) can be linearly approximated as follows,[9]

$$f_{lat} = \beta\frac{\dot{\eta}}{|\dot{\rho}|} \qquad f_{long} = \alpha\frac{\dot{\zeta}}{|\dot{\rho}|}$$

where $\alpha > 0$ and $\beta < 0$ are constants.

For real commercial WMRs, we can only control forward velocity *v* and angular velocity *w* instead of wheel torque. For pure rolling case, there is a mapping between v,w and $\dot\theta_1,\dot\theta_2$ as,

$$\begin{bmatrix} v \\ w \end{bmatrix} = \begin{bmatrix} r/2 & r/2 \\ r/2/b & -r/2/b \end{bmatrix} \begin{bmatrix} \dot\theta_1 \\ \dot\theta_2 \end{bmatrix}. \quad (31)$$

However, when the pure rolling is relaxed and slips are introduced, this mapping does not have physical meaning anymore. Now when we give command v and w to the robot, we are essentially giving command $\dot\theta_1$ and $\dot\theta_2$ derived from mapping (31) to control the robot dynamics (23) instead of robot kinematics. Now in the following steps, we consider $\dot\theta_1$ and $\dot\theta_2$ as control inputs and design feedback law to control dynamic model as in (23).

The kinematic model of the robot is

$$\begin{bmatrix} \dot x_0 \\ \dot y_0 \\ \dot\phi_0 \end{bmatrix} = \begin{bmatrix} \cos\phi & -\sin\phi & 0 \\ \sin\phi & \cos\phi & 0 \\ 0 & 0 & 1 \end{bmatrix} \begin{bmatrix} v \\ \dot\eta \\ w \end{bmatrix} \quad (32)$$

where x_0, y_0, ϕ_0 are configuration of point P_0 in Fig.1, and the dynamic model is, as in (25),

$$\overline{\overline{M}}\dot{\overline{v}} + \overline{\overline{C}}(\overline{q},\dot{\overline{q}})\overline{v} = \overline{\overline{F}}\ .$$

When we define new state variables z_1, z_2, z_3, z_4, z_5, z_6 as

$$\begin{aligned} z_1 &= -x_0\sin\phi + y_0\cos\phi - \frac{bB}{D}\phi \\ z_2 &= x_0\cos\phi + y_0\sin\phi \\ z_3 &= \phi \\ [z_4, z_5, z_6]^T &= \overline{\overline{M}}\overline{v} \end{aligned} \quad (33)$$

where

$$\overline{\overline{M}}^{-1} = \begin{bmatrix} A & -bB & bB \\ -bB & E-bD & E+bD \\ bB & E+bD & E-bD \end{bmatrix},$$ (A,B,D,E are constants)

$$\overline{\overline{C}} = \frac{m_r}{2}\dot\phi \begin{bmatrix} 0 & 1 & 1 \\ -1 & 0 & d/b \\ -1 & -d/b & 0 \end{bmatrix} + m_w\dot\phi \begin{bmatrix} 0 & 1 & 1 \\ -1 & 0 & 0 \\ -1 & 0 & 0 \end{bmatrix},$$

and noting that

$$\begin{bmatrix} \dot\eta \\ v \\ w \end{bmatrix} = \begin{bmatrix} 1 & 0 & 0 \\ 0 & 1/2 & 1/2 \\ 0 & 1/2/b & -1/2/b \end{bmatrix} \begin{bmatrix} \dot\eta \\ \dot\rho_1 \\ \dot\rho_2 \end{bmatrix}, \quad (34)$$

we will have a new set of equations as

$$\dot z_1 = (A + \frac{bBB}{D} + Bz_2)z_4 + Dz_2(z_5 + z_6) \quad (35)$$

$$\dot z_2 = -B(z_1 + \frac{bB}{D}z_3)z_4 + (E - Dz_1 - bBz_3)z_5 + (E + Dz_1 + bBz_3)z_6 \quad (36)$$

$$\dot z_3 = -Bz_4 - Dz_5 + Dz_6 \quad (37)$$

$$\begin{aligned} \dot z_4 = &-(-Bz_4 - D(z_5 - z_6))(m_r + 2m_w)E(z_5 + z_6) + \\ &\beta(Az_4 - bB(z_5 - z_6))(\left|-bBz_4 + E(z_5+z_6) - bD(z_5 - z_6)\right|^{-1} \\ &+ \left|bBz_4 + E(z_5+z_6) + bD(z_5 - z_6)\right|^{-1}) \end{aligned} \quad (38)$$

$$\dot z_5 = u_1 \quad (39)$$

$$\dot z_6 = u_2 \quad (40)$$

where $u_1 = \frac{1}{2}(m_r + 2m_w)\dot\eta\dot\phi - \frac{m_r d}{2b}\dot\rho_2\dot\phi + \alpha\frac{r\dot\theta_1 - \dot\rho_1}{\dot\rho_1}$, (41)

$$u_2 = \frac{1}{2}(m_r + 2m_w)\dot\eta\dot\phi + \frac{m_r d}{2b}\dot\rho_1\dot\phi + \alpha\frac{r\dot\theta_2 - \dot\rho_2}{\dot\rho_2} \quad (42)$$

As stated in [15], such a system cannot be exponentially stabilized at an equilibrium using smooth feedback, and it is not asymptotically stabilizable to a desired equilibrium solution using time-invariant continuous feedback. Define $z=(z_1,z_2,z_3,z_4,z_5,z_6)^T \in \mathbf{M}$, and the set of equilibrium manifold $\mathbf{M}^e=\{z\in \mathbf{M} | z_4=z_5=z_6=0\}$, follow [15] and it is easy to prove that the system described by (35)-(40) is strongly accessible on $\mathbf{M}$, and it is small-time locally controllable at any equilibrium $z^e \in \mathbf{M}^e$.

Now we design a time-invariant discontinuous feedback control law for the above system. We focus only on the problem of feedback stabilization to the origin, i.e. $z^e=0$.

3.1. Stabilization of reduced system

We first study the following reduced order system, which is obtained by considering the subsystem (35)-(38), letting (z_5+z_6, z_5-z_6) be the control variables (v_1,v_2):

$$\dot z_1 = (A + \frac{bBB}{D} + Bz_2)z_4 + Dz_2 v_2 \quad (43)$$

$$\dot z_2 = -B(z_1 + \frac{bBz_3}{D})z_4 + Ev_1 - D(z_1 + \frac{bBz_3}{D})v_2 \quad (44)$$

$$\dot z_3 = -Bz_4 - Dv_2 \quad (45)$$

$$\begin{aligned} \dot z_4 = &-(-Bz_4 - Dv_2)(m_r + 2m_w)Ev_1 \\ &+ \beta(Az_4 - bBv_2)(\left|-bBz_4 + Ev_1 - bDv_2\right|^{-1} + \left|bBz_4 + Ev_1 + bDv_2\right|^{-1}) \end{aligned} \quad (46)$$

Consider above reduced system (43)-(46). Restricting consideration to $z_3 \neq 0$, we apply the σ-process in [11]

$$y_1 = z_3, x_2 = z_2, x_3 = \frac{z_1}{z_3}, x_4 = \frac{z_4}{z_3}$$

to obtain

$$\dot y_1 = -By_1x_4 - Dv_2 \quad (47)$$

$$\dot x_2 = Ev_1 - B(y_1x_3 + \frac{bBy_1}{D})y_1x_4 - D(y_1x_3 + \frac{bBy_1}{D})v_2 \quad (48)$$

$$\dot x_3 = (A + \frac{bBB}{D} + Bx_2)x_4 + \frac{Dx_2v_2}{y_1} + \frac{x_3}{y_1}(By_1x_4 + Dv_2) \quad (49)$$

$$\begin{aligned} \dot x_4 = &-\frac{1}{y_1}(-By_1x_4 - Dv_2)(m_r + 2m_w)Ev_1 \\ &+ \frac{\beta}{y_1}(Ay_1x_4 - bBv_2)(\left|-bBy_1x_4 + Ev_1 - bDv_2\right|^{-1} \\ &+ \left|bBy_1x_4 + Ev_1 + bDv_2\right|^{-1}) + \frac{x_4}{y_1}(By_1x_4 + Dv_2) \end{aligned} \quad (50)$$

We design the feedback law to be

$$v_1 = (-l_1x_2 - l_2x_3)/E\ , \quad (51)$$

$$v_2 = (k_1y_1 - By_1x_4)/D\ , \quad (52)$$

where $k_1>0$ and l_1, l_2 are the gains, to derive the reduced closed loop system

$$\dot y_1 = -k_1y_1 \quad (53)$$

$$\dot x_2 = -l_1x_2 - l_2x_3 - k_1(x_3 + \frac{bB}{D})y_1{}^2 \quad (54)$$

$$\dot{x}_3 = (A + \frac{bBB}{D})x_4 + k_1 x_2 + k_1 x_3 \tag{55}$$

$$\dot{x}_4 = -k_1(m_r + 2m_w)(l_1 x_2 + l_2 x_3) + k_1 x_4 + \beta((A + \frac{bBB}{D})x_4 - k_1 \frac{bB}{D})(|\gamma_1|^{-1} + |\gamma_2|^{-1}) \tag{56}$$

where $\gamma_1 = -l_1 x_2 - l_2 x_3 - k_1 b y_1$ and $\gamma_2 = -l_1 x_2 - l_2 x_3 + k_1 b y_1$.

The x-dynamics can be rewritten as

$$\dot{x} = (A_1 + A_2(t))x + h_1(t) \tag{57}$$

where

$$A_1 = \begin{bmatrix} -l_1, & -l_2, & 0 \\ k_1, & k_1, & A + \frac{bBB}{D} \\ -k_1 l_1(m_r + 2m_w), & -k_1 l_2(m_r + 2m_w), & k_1 + \beta(A + \frac{bBB}{D})(|\gamma_1|^{-1} + |\gamma_2|^{-1}) \end{bmatrix} \tag{58}$$

$$A_2(t) = \begin{bmatrix} 0 & -k_1 {x_{10}}^2 e^{-2k_1 t} & 0 \\ 0 & 0 & 0 \\ 0 & 0 & 0 \end{bmatrix}, \tag{59}$$

$$h_1(t) = [-k_1 \frac{bB}{D} {y_{10}}^2 e^{-2k_1 t},\ 0,\ -k_1 \beta \frac{bB}{D}(|\gamma_1|^{-1} + |\gamma_2|^{-1})]^T. \tag{60}$$

It can be easily seen that if $0<l_1<l_2$ and $k_1 + \beta(A + \frac{bBB}{D})(|\gamma_1|^{-1} + |\gamma_2|^{-1}) < 0$, the eigenvalues of matrix A_1 can be assigned arbitrarily on the left side of phase plane. Note that $k_1 + \beta(A + \frac{bBB}{D})(|\gamma_1|^{-1} + |\gamma_2|^{-1}) < 0$ can be satisfied when set an upper bound for the robot's forward velocity. Clearly, the y_1-dynamics is globally exponentially stable at y_1=0. Moreover, since matrix A_2(t) and h_1(t) go to zero as $t \to \infty$ (note that $(|\gamma_1|^{-1} + |\gamma_2|^{-1})$, representing the lateral traction term, will disappear when z_3 converges to zero), and

$$\int_0^\infty \|A_2(t)\| dt < \infty,\ \int_0^\infty \|h_1(t)\| dt < \infty,$$

the x dynamics can also be globally exponentially stable at the origin x=0 when matrix A_1 is a Hurwitz matrix [26].

Note that in the (z_1,z_2,z_3,z_4) coordinates the control law takes the form of

$$\mathrm{v}_1(z_1, z_2, z_3, z_4) = (-l_1 z_2 - l_2 \frac{z_1}{z_3})/E \tag{61}$$

$$\mathrm{v}_2(z_1, z_2, z_3, z_4) = (k_1 z_3 - B z_4)/D \tag{62}$$

and the reduced closed-loop system becomes

$$\dot{z}_1 = (A + \frac{bBB}{D})z_4 + k_1 z_2 z_3 \tag{63}$$

$$\dot{z}_2 = -l_1 z_2 - l_2 \frac{z_1}{z_3} - k_1 z_3 (z_1 + \frac{bB}{D} z_3) \tag{64}$$

$$\dot{z}_3 = -k_1 z_3 \tag{65}$$

$$\dot{z}_4 = k_1 z_3 (m_r + 2m_w)(-l_1 z_2 - l_2 \frac{z_1}{z_3}) + \beta((A + \frac{bBB}{D})z_4 - k_1 \frac{bB}{D} z_3)\left(\left|-l_1 z_2 - l_2 \frac{z_1}{z_3} - k_1 b z_3\right|^{-1} + \left|-l_1 z_2 - l_2 \frac{z_1}{z_3} + k_1 b z_3\right|^{-1}\right) \tag{66}$$

It is easily to show that both the trajectory ($z_1(t)$,$z_2(t)$,$z_3(t)$,$z_4(t)$) and (v_1(t),v_2(t)) are bounded for all $t \geq 0$ and converges exponentially to zero. Moreover, the control law (61)-(62) drives the system (63)-(66) to the origin, while avoiding the set

$$N = \{(z_1, z_2, z_3, z_4) \mid z_3 = 0, (z_1, z_2, z_4) \neq 0\}.$$

3.2. *Stabilization of the complete system*

Now we study the problem of asymptotic stabilization of the complete system (35)-(40), with u_1 and u_2, instead of x_5 and x_6, as control inputs. However, the integrator back-stepping approach developed for smooth systems cannot be directly applied here to derive control inputs due to the discontinuous nature of the system.

Consider the controllers satisfying the following equations:

$$u_1(z) + u_2(z) = -K(z_5 + z_6 - \mathrm{v}_1(z_1, z_2, z_3, z_4)) + s_1(z) \tag{67}$$

$$u_1(z) - u_2(z) = -L(z_5 - z_6 - \mathrm{v}_2(z_1, z_2, z_3, z_4)) + s_2(z) \tag{68}$$

where v_1 and v_2 are feedback laws for reduced system, and s_1 and s_2 correspond to their time derivatives along (35)-(40)

$$s_1(z) = \frac{1}{E}(l_1(-B(z_1 + \frac{bB}{D} z_3)z_4 + E(z_5 + z_6) - (Dz_1 + bBz_3)(z_5 - z_6)) + \frac{l_2}{z_3}((A + \frac{bBB}{D} + Bz_2)z_4 + Dz_2(z_5 + z_6)) + l_2 \frac{z_1}{z_3}(Bz_4 + D(z_5 - z_6)))$$

$$s_2(z) = \frac{1}{D}(-k_1(Bz_4 + D(z_5 - z_6)) + B(Bz_4 + D(z_5 - z_6))(m_r + 2m_w) E(z_5 + z_6) - B\beta(Az_4 - bB(z_5 - z_6)) (\left|-bBz_4 + E(z_5 + z_6) - bD(z_5 - z_6)\right|^{-1} + \left|bBz_4 + E(z_5 + z_6) + bD(z_5 - z_6)\right|^{-1}))$$

The idea is to implement the control law in (61)(62) through the integrators by choosing gains K and L appropriately.

Consider the coordinate transformation

$$y_1 = z_3, x_2 = z_2, x_3 = \frac{z_1}{z_3}, x_4 = \frac{z_4}{z_3},$$

$$w_1 = z_5 + z_6 + (l_1 z_2 + l_2 \frac{z_1}{z_3})/E, \quad w_2 = z_5 - z_6 - (k_1 z_3 - Bz_4)/D$$

Then, it can be shown that the close-loop system can be written as

$$\dot{y}_1 = -k_1 y_1 - D w_2 \tag{69}$$

$$\dot{x} = (A_1 + \widetilde{A}_2(t))x + h_2(t) \tag{70}$$

$$\dot{w}_1 = -K w_1 \tag{71}$$

$$\dot{w}_2 = -L w_2 \tag{72}$$

where A_1 is the matrix given by (58) and

$$\widetilde{A}_2(t) = \begin{bmatrix} 0 & r_1(t) & 0 \\ r_2(t) & r_2(t) & 0 \\ -l_1(m_r + 2m_w)r_2(t) & -l_2(m_r + 2m_w)r_2(t) & r_2(t) \end{bmatrix}$$

$$r_1(t) = -(y_{10} e^{-k_1 t} + \frac{E w_{20}}{L - k_1} e^{-Lt})(k_1 y_{10} e^{-k_1 t} + \frac{LD w_{20}}{L - k_1} e^{-Lt})$$

$$r_2(t) = D(y_{10} e^{-k_1 t} + \frac{D w_{20}}{L - k_1} e^{-Lt})^{-1} w_{20} e^{-Lt}$$

$$h_2(t) = [-k_1 \frac{bB}{D} y_{10}{}^2 e^{-2k_1 t} - bBy_{10} w_{20} e^{-(L+k_1)t} + Ew_{10}e^{-Kt},\ 0,$$

$$(m_r + 2m_w)Ew_{10}e^{-Kt}(k_1 + r_2(t)) - \beta \frac{bB}{D}(k_1 + r_2(t))(\frac{1}{|\gamma_1{}'|} + \frac{1}{|\gamma_2{}'|})]^T$$

where $\gamma_1{}' = -l_1 x_2 - l_2 x_3 - k_1 b x_1 + Ew_{10}e^{-Kt} - bDw_{20}e^{-Lt}$

and $\gamma_2{}' = k_1 b x_1 - l_1 x_2 - l_2 x_3 + Ew_{10}e^{-Kt} + bDw_{20}e^{-Lt}$.

The (y_1,w_1,w_2)-dynamics is globally exponentially stable at $(y_1,w_1,w_2)=(0,0,0)$. It can be shown that if $K>k_1$ and $y_{10}w_{10} \geq 0$ (i.e. $z_{30}(z_{50} + z_{60} + l_1 z_{20}/E) + l_2 z_{10}/E \geq 0$) then $\tilde{A}_2(t)$ and $h_2(t)$ go to zero as $t \to \infty$ and

$$\int_0^\infty \left\|\tilde{A}_2(t)\right\| dt < \infty,\ \int_0^\infty \left\|h_2(t)\right\| dt < \infty.$$

Thus, for any initial condition $(y_{10},x_0,w_{10},w_{20})$ satisfying $y_{10} \neq 0$ and $y_{10}w_{10} \geq 0$, both the trajectory $(y_1(t), x(t), w_1(t), w_2(t))$ and the control $(u_1(t), u_2(t))$ are bounded for all $t \geq 0$ and converge exponentially to zero. Furthermore, the trajectory $(x_1(t), x_2(t), x_3(t), x_4(t), x_5(t), x_6(t))$ is bounded for all $t \geq 0$ and converges exponentially to zero.

4 Simulation Results

We present simulation results to validate our discontinuous controller on the WMR model that include slip dynamics. For the simulation task the WMR parameters (refer Fig.1) are as follows: b=0.24m; d=0.05m; r=0.095m; m_r=16kg; m_w=0.5kg; I_{rz}=0.537; I_{wy}=0.0023kgm^2; I_{wz}=0.0011kgm^2. We apply our proposed controller to the stabilization problem that is subject to both lateral and longitudinal slips. The traction curve slope parameters are $\alpha = 20, \beta = -12$.

4.1 *Example*

We set the origin as desired configuration and simulate the problem with the initial position of the robot $[x_0, y_0, \phi_0] = [-2, -1, 0]$, initial forward velocity $\upsilon_0 = 0$ and initial angular velocity $\omega_0 = 0$. The control gains are: K=0.5, L=0.5, k_1=0.044, l_1=1, l_2=2.

Fig. 5 is the robot trajectory converging to the origin. Fig. 6 is the robot configuration, where we observe that the robot is able to converge to the origin with monotonically decreasing ϕ. The lateral and longitudinal slip velocities are shown in Fig. 7 and Fig.8. It can be seen that the left side wheel needs more slip to generate more traction than the right wheel for the robot to take a right turn. Fig. 9 shows the control inputs $\dot{\theta}_1$ and $\dot{\theta}_2$, respectively. We observe that both the control inputs are bounded and converge to zero asymptotically.

5 Conclusion

In this paper, we model the WMR in a way that the pure rolling constraint is relaxed and wheel dynamics with slip is considered. We develop translational wheel dynamic model with slip and introduce the dynamics into overall robot dynamics. By the traction model used in this paper, translational wheel dynamics is connected with rotational wheel dynamics, thus the entire robot dynamic system becomes a third order system. Wheel slip phenomenon is captured and at the same time accommodated. We develop a discontinuous controller, in which exponential convergence of the system is guaranteed. We apply this controller to point stabilization and its effectiveness is validated in simulations. In our future work, we plan to develop tracking controller for single robot and for robot formation with slips.

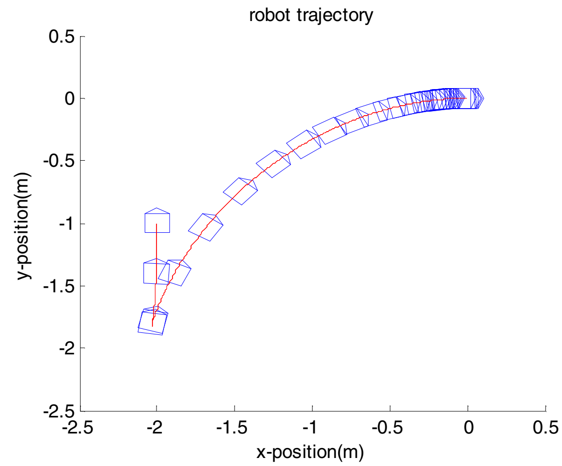

Fig. 5 Robot trajectory

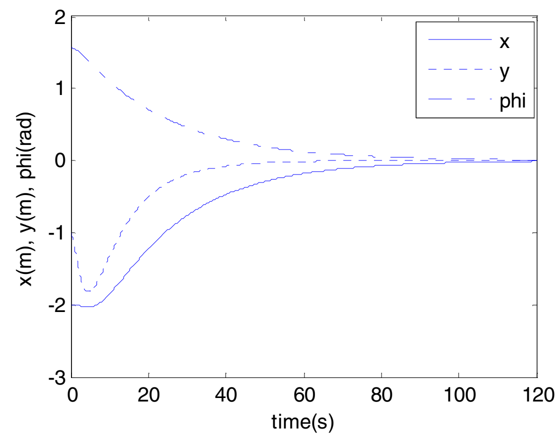

Fig. 6 Robot configuration

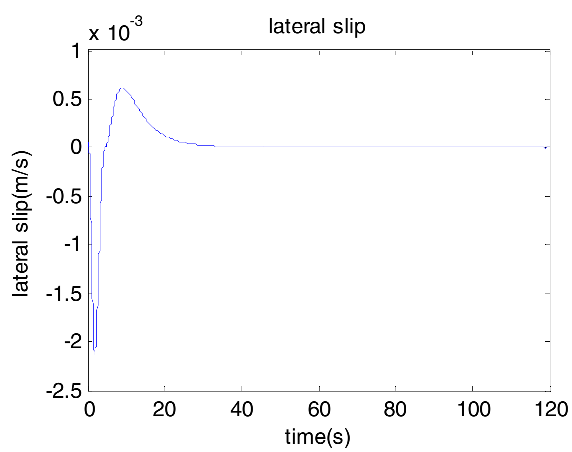

Fig. 7 Lateral slip velocity

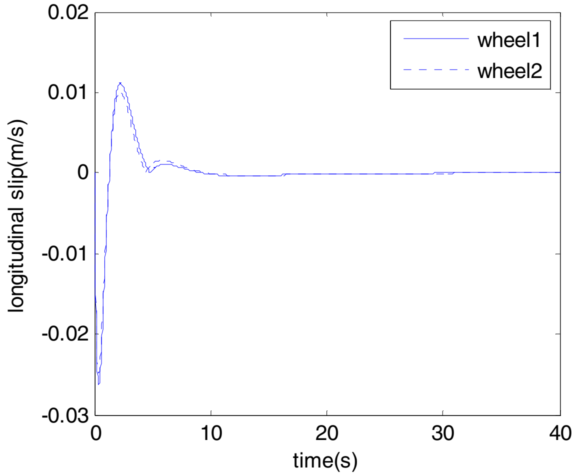

Fig. 8 Longitudinal slip velocity for wheel1 and wheel2 in the first 40 seconds

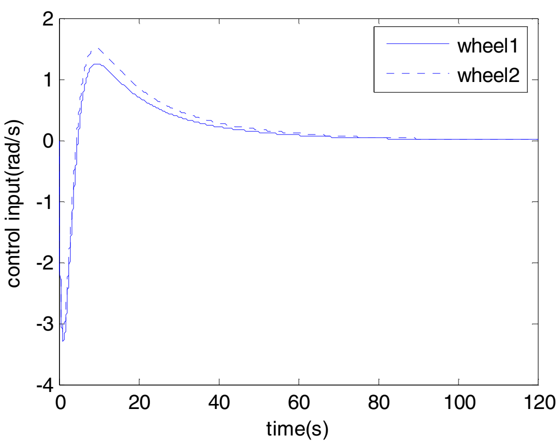

Fig. 9 Control inputs for wheel1 and wheel2

REFERENCES

[1] Motte I., Campion I., "A slow manifold approach for the control of mobile robots not satisfying the kinematic constraints", *IEEE Trans. on Robotics and Automation*, Vol. 16, No. 6, 2000, pp. 875-880.

[2] Lin W.-S., Chang L.-H., Yang P.-C., "Adaptive critic anti-slip control of wheeled autonomous robot", *Control Theory & Applications, IET*, Vol. 1, Issue 1, 2007, pp: 51 – 57.

[3] Tarokh M., McDermott G.J., "Kinematics modeling and analyses of articulated rover", *IEEE Trans. on Robotics*, Vol. 21, No.4, 2005, pp: 539-553.

[4] Volpe R., "Navigation results from desert field tests of the Rocky 7 Mars rover prototype", *The Int. Journal of Robotics Research*, Vol. 18, No. 7, 1999, pp: 669-683.

[5] Dixon W.E., Dawson D.M., Zergeroglu E., "Robust control of a mobile robot system with kinematic disturbance", *IEEE Int. Conference on Control Applications*, 2000, pp: 437-442.

[6] Balakrishna R. and Ghosal A., "Modeling of slip for wheeled mobile robot", *IEEE Trans. on Robotics and Automation*, Vol. 11, No. 1, 1995, pp: 126-132.

[7] Jung S., Hsia T.C., "Explicit lateral force control of an autonomous mobile robot with slip", *IEEE/RSJ Int. Conf. on Intelligent Robots and Systems*, IROS 2005, pp: 388 – 393.

[8] Stonier D., Hyoung C. Se-, Sung-Lok C., Kuppuswamy N.S., Jong-Hwan K., "Nonlinear slip dynamics for an omni-wheel mobile robot platform", *IEEE Int. Conf. on Robotics and Automation*, 2007, pp: 2367 – 2372.

[9] Jeren Ploeg, Hanno E. Schouten and Henk Nijmeijer, "Control Design for a Mobile Robot Including Tire Behavior", *2008 IEEE Intelligent Vehicles Symposium*, Eindhoven, The Netherlands, June 4-6, 2008, pp. 240-245.

[10] Naim Sidek and Nilanjan Sarkar, "Dynamic Modeling and Control of Nonholonomic Mobile Robot with Lateral Slip", *2008 IEEE Third International Conference on ICONS 08*, pp. 35-40.

[11] Takanori Fukao, Hiroshi Nakagawa and norihiko Adachi, "Adaptive Tracking Control of a Nonholonomic Mobile Robot", *2000 IEEE Trans. on Robotics and Automation*, vol. 16, No. 5, pp: 609-615.

[12] R. Fierro and F. L. Lewis, "Control of a Nonholonomic Mobile Robot: Backstepping Kinematics into Dynamics", Journal of Robotics Systems, vol. 14, No. 3, pp: 149-163, 1997.

[13] Zhong-ping Jiang and Henk Nijmeijer, "Tracking Control of Mobile Robots: A Case Study in Backstepping", *Automatica*, vol. 33, No. 7, pp: 1393-1399, 1997.

[14] Khac Duc Do, Zhong-Ping Jiang and Jie Pan, "A Global Output-Feedback Controller for Simultaneous Tracking and Stabilization of Unicycle-Type Mobile Robots", *IEEE Trans. on Robotics and Automation*, vol. 20, No. 3, pp: 589-594, 2004.

[15] Mahmut Reyhanoglu, "Exponential Stabilization of an Underactuated Autonomous Surface Vessel", *Automatica*, Vol. 33, No. 12, pp: 2249-2254, 1997.

[16] Frederic Mazenc, Kristin Pettersen and Henk Nijmeijer, "Global Uniform Asymptotic Stabilization of an Underactuated Surface Vessel", *IEEE Trans. on Automatic Control*, Vol. 47, No. 10, 2002, pp: 1759-1762.

[17] Dong, Wenjie and Guo, Yi, "Global Time-Varying Stabilization of Underactuated Surface Vessel", *IEEE Trans. on Automatic Control*, Vol. 50, No. 6, 2005, pp: 859-864.

[18] Jawhar Ghommam, Faical Mnif, Abderraouf Benali and Nabil Derbel, "Asymptotic Backstepping Stabilization of an Underactuated Surface Vessel", *IEEE Trans. on Control Systems Technology*, Vol. 14, No. 6, 2006, pp: 1150-1157.

[19] A. Behal, D. M. Dawson, W. E. Dixon and Y. Fang, "Tracking and Regulation Control of an Underactuated Surface Vessel With Nonintegrable Dynamics", *IEEE Trans. on Automatic Control*, Vol. 47, No. 3, pp: 495-500, 2002.

[20] Erjen Lefeber, Kristin Pettersen and Henk Nijmeijer, "Tracking Control of an Underactuated Ship", *IEEE Trans. on Control Systems Technology*, Vol. 11, No. 1, 2003, pp: 52-61.

[21] Yun X, Yamamoto Y., "Internal dynamics of a wheeled mobile robot", *IEEE/RSJ Int. Conf. on Intelligent Robots and Systems*, Yokohama Japan, 1993, pp: 1288-1294.

[22] Sarkar N., Yun X., "Control of mechanical systems with rolling constraints: Application to the dynamic control of mobie robots", *Int. Journal of Robotics Research*, Vol. 31, 1994, pp: 55-69.

[23] Kumar V., Wellman P., Krovi V., Appl. No.: 239,951, Filed: May 9, 1994, Granted: May 7, 1996, Adaptive mobility system, United States Patent 5,513,716.

[24] Salerno A., Angeles J., "A new family of two-heeled mobile robots: modeling and controllability", *IEEE Transactions on Robotics*, Vol. 23, Issue 1, 2007, pp: 169 – 173.

[25] Ward C.C., Iagnemma K., "Model-based wheel slip detection for outdoor mobile robots", *IEEE Int. Conf. on Robotics and Automation*, 2007, pp: 2724 – 2729."

[26] Slotine, J.-J. E. And W. Li, *Applied nonlinear Control*, Prentice-Hall, Englewood Cliffs, NJ.